Resource

SOURCE DATA | TRANSPARENT PROCESS

THE EMBO JOURNAL

Co-regulation proteomics reveals substrates and mechanisms of APC/C-dependent degradation

Sasha A Singh[1,2,3,4,†,§], Dominic Winter[1,2,‡,§], Marc Kirchner[1,2,§], Ruchi Chauhan[2,3,4,§], Saima Ahmed[2], Nurhan Ozlu[5], Amit Tzur[6], Judith A Steen[2,3,4,¶,*] & Hanno Steen[1,2,¶,**]

Abstract

Using multiplexed quantitative proteomics, we analyzed cell cycle-dependent changes of the human proteome. We identified >4,400 proteins, each with a six-point abundance profile across the cell cycle. Hypothesizing that proteins with similar abundance profiles are co-regulated, we clustered the proteins with abundance profiles most similar to known Anaphase-Promoting Complex/Cyclosome (APC/C) substrates to identify additional putative APC/C substrates. This protein profile similarity screening (PPSS) analysis resulted in a shortlist enriched in kinases and kinesins. Biochemical studies on the kinesins confirmed KIFC1, KIF18A, KIF2C, and KIF4A as APC/C substrates. Furthermore, we showed that the APC/C^{CDH1}-dependent degradation of KIFC1 regulates the bipolar spindle formation and proper cell division. A targeted quantitative proteomics experiment showed that KIFC1 degradation is modulated by a stabilizing CDK1-dependent phosphorylation site within the degradation motif of KIFC1. The regulation of KIFC1 (de-)phosphorylation and degradation provides insights into the fidelity and proper ordering of substrate degradation by the APC/C during mitosis.

Keywords dynamic proteomics; protein profile similarity screening; quantitative proteomics; TMT-labeling; ubiquitination-dependent protein degradation
Subject Categories Cell Cycle; Methods & Resources; Post-translational Modifications, Proteolysis & Proteomics
DOI 10.1002/embj.201385876 | Received 3 June 2013 | Revised 5 December 2013 | Accepted 6 December 2013 | Published online 6 February 2014
EMBO Journal (2014) 33, 385–399

Introduction

The mammalian cell cycle is controlled by the distinct quantitative oscillations of a subset of proteins that are ubiquitinated by the E3 ligase Anaphase-Promoting Complex/Cyclosome (APC/C), and subsequently degraded by the proteasome (Hadwiger *et al*, 1989; Murray & Kirschner, 1989; Murray *et al*, 1989; Richardson *et al*, 1989; King *et al*, 1996; Peters, 2006). Over the last two decades, the study of APC/C and its targets resulted in the identification of a set of proteins whose APC/C-mediated turnover is critical for the ordered progression through mitosis and the cell cycle in general. Strategies to identify and validate novel APC/C targets have always been a matter of great interest particularly due to the strong link between cell cycle regulation and human diseases, most notably cancer. To date, systematic screens for APC/C targets typically rely on laborious *in vitro*-based methods (McGarry & Kirschner, 1998; Ayad *et al*, 2003, 2005). Recent high-throughput methods have greatly simplified the search for APC/C targets (Merbl & Kirschner, 2009; Kim *et al*, 2011; Wagner *et al*, 2011); however, the *in vitro*-based screen designs for ubiquitination without the context of degradation are not readily confirmed. Understanding APC/C-mediated regulation of mitosis remains critical because of the close relationship between malignant cell division, genomic instability and tumorigenesis (Nakayama & Nakayama, 2006).

Here we exploit the versatility of multiplexed quantitative proteomic strategies to develop an efficient *in vivo*-based strategy for the identification of novel APC/C substrates and also to dissect the mechanisms by which the degradation of these APC/C substrates are regulated. We conducted a time-course experiment to identify substrates degraded by the APC/C during mitosis. The basis for the identification of novel APC/C substrates by co-regulation proteomics resembles the approach taken in many transcriptomics studies in which transcripts with similar quantitative profiles are identified to find co-regulated genes (e.g. Brady *et al*, 2007a,b; Reinhold *et al*,

1 Department of Pathology, Boston Children's Hospital and Harvard Medical School, Boston, MA, USA
2 Proteomics Center at Boston Children's Hospital, Boston, MA, USA
3 Department of Neurology, Boston Children's Hospital and Harvard Medical School, Boston, MA, USA
4 F.M. Kirby Neurobiology Center, Boston Children's Hospital, Boston, MA, USA
5 College of Sciences, Koç University, Istanbul, Turkey
6 The Mina and Everard Goodman Faculty of Life Sciences and Institute of Nanotechnology and Advanced Materials, Bar-Ilan University, Ramat-Gan, Israel
*Corresponding author. Tel: +1 617 919 2450; Fax: +1 617 919 2771; E-mail: judith.steen@childrens.harvard.edu
**Corresponding author. Tel: +1 617 919 2629; Fax: +1 617 730 0148; E-mail: hanno.steen@childrens.harvard.edu
§These authors should be considered shared first author.
¶These authors contributed equally to the work.
†Present address: Division of Cardiovascular Medicine, Brigham and Women's Hospital, Harvard Medical School, Boston, MA, USA
‡Present address: Institute of Biochemistry and Molecular Biology, University of Bonn, Bonn, Germany

2011). The premise is that genes involved in related pathways are co-regulated at the transcriptional level, such that novel transcripts whose profiles are similar to those of known function are likely to function similarly. These genes are then followed up in-depth.

Following this idea, we employed a 6-plex tandem mass tagging (TMT)-based quantitative proteomic strategy (Dayon *et al*, 2008) that provides relative endogenous protein abundances. Synchronized cells were sampled before, during and post-mitosis (Fig 1A), where the APC/C displays activity specifically from prometaphase to late G1 phase (Draetta *et al*, 1989; King *et al*, 1995; Clute & Pines, 1999; Zou *et al*, 1999; Hagting *et al*, 2002). Apart from the "prototypic" APC/C substrates, SECURIN and CYCLIN B, approximately 70 additional cell cycle-dependent APC/C substrates have since been identified, and in most cases, their respective APC/C co-activators, CDC20 or CDH1. Most of these substrates display a distinct protein abundance profile during the cell cycle which has become a hallmark for APC/C-dependent regulation (Fig 1A).

We hypothesized that all proteins ubiquitinated by the APC/C, and then degraded by the proteasome in a cell cycle-dependent manner, would show similar abundance profiles over the course of the cell cycle. Thus, in order to identify novel substrates of the APC/C, we determined reference protein abundance profiles based on known APC/C substrates and compared them to the abundance profiles of all the other proteins we detected. This approach generated a shortlist of putative APC/C substrates, some of which were confirmed using the conventional *in vitro* degradation assays.

Selecting the newly identified APC/C substrate KIFC1 for detailed follow-up studies, we used the FLEXIQuant strategy, which was developed in our lab (Singh *et al*, 2009), to profile the cell cycle-dependent dynamics of the post-translational modifications (PTMs) of KIFC1. These experiments revealed insights into the interplay between phosphorylation and APC-dependent degradation, pointing towards a more common, though underappreciated mechanism for timing the degradation of APC/C substrates.

Results

Our first goal was to generate synchronous cell populations at 6 different points along the cell cycle. To this end, cells were synchronized using the double thymidine block approach since it shows less pleiotropic effects than other commonly applied nocodazole/taxol-based synchronization protocols, which activate the mitotic checkpoints (Steen *et al*, 2008). Synchronization and validation details can be found in Fig 1A and Supplementary Fig S1. After lysis of cell pellets from each time point, proteins were trypsinized in solution. The resulting peptides from each time point were subsequently labeled with one of six TMT labels and combined into one sample (Fig 1A). The peptide mixtures were fractionated into 24 fractions by isoelectric focusing prior to LC-MS/MS analysis. To minimize undersampling of this complex sample, thereby ensuring a robust dataset, three biological replicates were analyzed in triplicate by LC/MS resulting in 216 LC/MS/MS runs matching 264,386 MS/MS spectra identifying 44,085 unique peptides at a 1% false discovery rate (FDR) (Supplementary Table S1). For subsequent protein grouping, we required a 1% FDR cut-off and a minimum of at least two unique peptides with complete TMT-reporter ion traces. Applying these criteria, this experiment identified and quantified 4,470 non-redundant proteins (Supplementary Table S1). Of these 4,470 proteins, 95% had three or more matched MS/MS spectra and 78% had three or more assigned unique peptides, which is important for robust quantification. MS/MS spectra derived from two known APC/C substrates, NUSAP1 and TPX2 are displayed in Fig 1B and C. The TMT reporter ions of these examples shown in the insets display the canonical abundance profile for an APC/C substrate with an initial increase in abundance that peaks between early to mid-mitosis, followed by a marked decrease well into G1. In contrast, the unregulated protein GAPDH shows no change in overall abundance (Fig 1D).

To examine further the robustness of the data, the following two metrics were evaluated: (i) the number of known APC/C substrates identified and (ii) the reproducibility of the TMT-based quantification. In our data set, we identified 24 known APC/C substrates corresponding to approximately 30% of the proteins known to be degraded by the APC/C. The very good reproducibility was confirmed by extracting all complete TMT-based peptide abundance profiles from the MS/MS spectra associated with NUSAP1 (24 complete peptide abundance profiles, Fig 1E), TPX2 (55 complete peptide abundance profiles, Fig 1F), and the "house-keeping" protein GADPH (371 complete peptide abundance profiles, Fig 1G), with the red trace corresponding to the mean profile, i.e. the respective protein abundance profile. The NUSAP1 and TPX2 profiles clearly represent the canonical abundance profile for APC/C substrates in contrast to GAPDH serving as negative control.

To identify co-regulated proteins in the quantitative proteomics datasets, a clustering analysis was performed using the protein abundance profiles. We adapted our previously reported strategy for screening protein profile similarities (Kirchner *et al*, 2010) to identify proteins whose abundance profiles resemble those of known APC/C substrates (Fig 2A). We used the normalized reporter ion traces from all MS/MS spectra to generate abundance profiles for each protein (Fig 2A, Steps 1 and 2). Next, the profiles of the identified known APC/C substrates were extracted. In our dataset, 17 of 24 identified known APC/C substrates, showed the canonical abundance profile for APC/C substrates, i.e. an initial increase during G2 phase followed by marked decrease in abundance, reaching the lowest level in G1 phase (Fig 2A, Step 3). Rather than execute our protein profile similarity screen on the average profile of all 17 APC/C substrates, we tested the robustness of our strategy by first assessing whether we could generate different APC/C reference clusters that would reflect different classes of APC/C substrates with slightly different abundance profiles. Using normal mixture modeling for model-based clustering which makes use of the Bayes factor and posterior model probabilities parameters, we established six as the optimum number of reference clusters (Fig 2A, Step 4). These different APC/C substrate references contained profiles that co-clustered into subgroups based on, for example, their respective apices and/or the steepness of their ascending and/or descending parts of their curves (Fig 2B). Cluster 1 contains only the cyclins, i.e. CDC20 substrates, whereas clusters 2–6 are predominated by CDH1 substrates (Fig 2B), indicating that the sub-cluster strategy was able to detect differences in degradation dynamics and to establish the cyclins as a unique CDC20 sub-cluster. We subsequently ranked all observed 4,470 protein profiles according to their similarity with the average profile of each reference cluster (Fig 2A, Step 5; Supplementary Table S2).

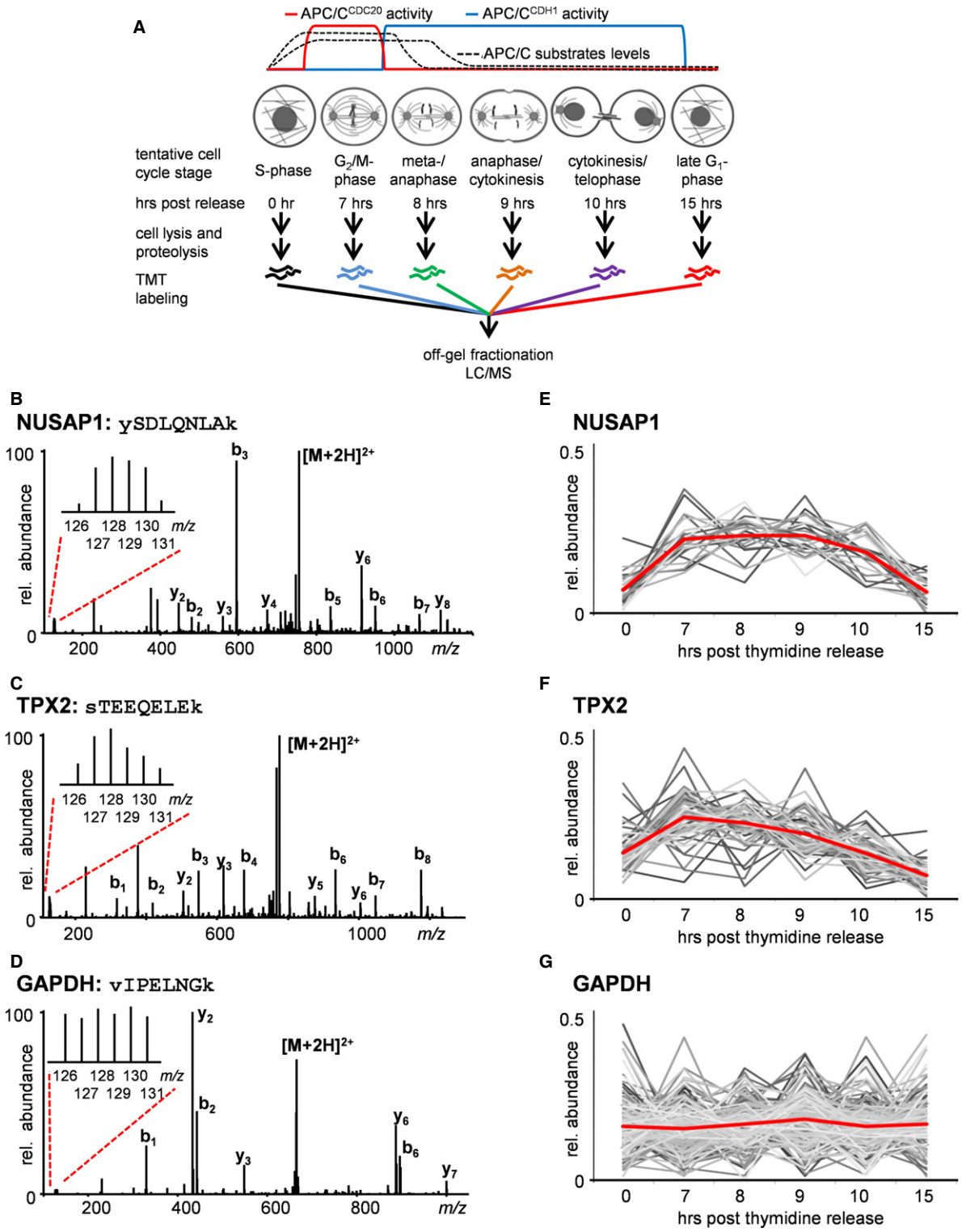

Figure 1. Overview of cell cycle proteomics experiments of synchronized HeLa cells.

A Upper panel: A schematic of APC/C activity with respect to prototypical substrate level profiles. APC/C can complex with either CDC20 or CDH1 as a co-activator. Lower panel: Workflow of the cell synchronization experiment and the subsequent TMT-based quantitative proteomics experiment.

B–D Representative MS/MS spectra and TMT reporter ion traces from the known APC/C substrates NUSAP1 (B), TPX2 (C) and from a non-APC/C substrate, GAPDH (D). Lower case amino acids indicate sites of TMT labels.

E–G The complete TMT-based peptide abundance profiles (after sum normalization) from all MS/MS spectra (peptide-spectrum matches) associated with NUSAP1 (E), TPX2 (F) and GAPDH (G), respectively, are shown in various shades of grey. The red traces indicate the mean.

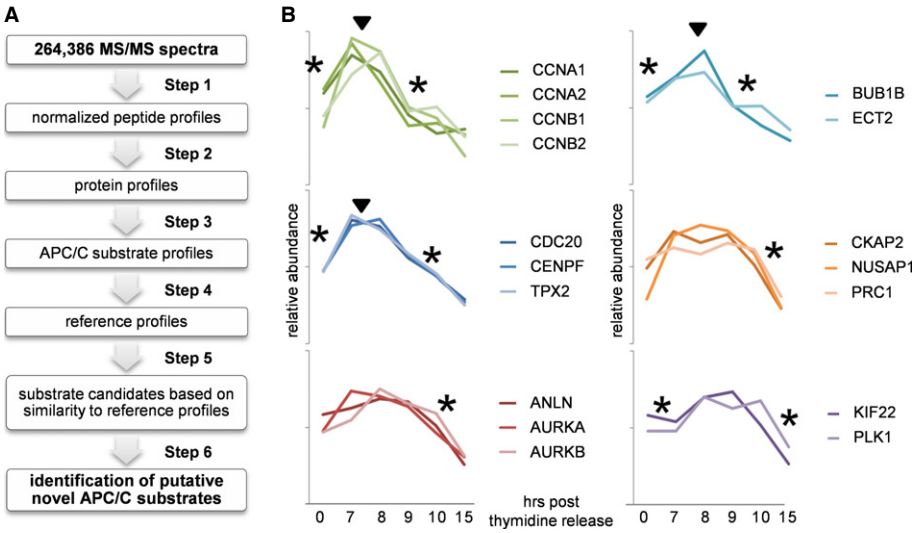

Figure 2. Protein clustering approach and results.

A The protein profile similarity screening workflow leading to the identification of novel APC/C substrates.

B The six APC/C reference clusters used in the co-regulation analysis as indicated in Steps 4 and 5 of (A). The proteins within each cluster are indicated. The arrowhead indicates a distinct abundance apex, and the asterisk indicates a differential steepness in the ascent and/or descent of the abundance profile.

To prioritize which of the best-matching proteins or protein families to study in more detail, a text analysis of the names of the proteins found in the 1st percentile of each reference cluster was performed (Fig 2A, Step 6 and Supplementary Fig S2). This analysis resulted in "kinase" (25 occurrences, rank 6) and "kinesin" (22 occurrences, rank 7) as the two most frequent protein family names following generic terms including "protein", "isoform", "similar", "flj", "cdna", "like", and "highly" co-occupying ranks 1–6. It is not surprising to find numerous kinases in the top percentile since several protein kinases have been described as APC/C substrates. It should be noted that given the variety of proteins (functions) identified to date for APC/C-substrates, it is likely that our dataset includes additional novel non-kinesin substrates that can be readily extracted either manually or with informatics approaches (Supplementary Table S2).

In contrast to the expected high number of kinase hits, the 18-fold enrichment of kinesins in the 1st percentile (between 2 and 5 kinesins per reference cluster, Fig 3A) in comparison to the entire dataset (20/4,470) was surprising. Only a single kinesin family member in higher eukaryotes, KIF22, had been described as an APC/C substrate previous to this study (Feine *et al*, 2007); in addition, two kinesins (KIP1 and CIN8) had already been described as substrates in yeast (Gordon & Roof, 2001; Hildebrandt & Hoyt, 2001). KIF22 was indeed within the 1st percentile in clusters 3, 4 and 6. The other kinesins within the top percentile of at least two clusters were KIF18A, KIF2C, KIF23, KIF14 and KIFC1. During the course of this work, KIF18A was described as an APC/C substrate by Sedgwick *et al*, independently confirming our co-regulation proteomics-based strategy and its results (Sedgwick *et al*, 2013).

Following the lead from the co-regulation analysis, we investigated the possibility that kinesins are indeed common APC/C substrates. To this end, we ranked the protein profiles of all identified kinesins in each reference cluster (Fig 2B) and subsequently calculated the median percentile for each kinesin (Fig 3A). To expand our short list of kinesins to be tested for APC/C-dependent degradation, we accepted all kinesins within the 5th percentile as potential APC/C substrates, thereby adding KIF13A and KIF4A to the list of candidate substrates. The mean TMT-based protein profiles for the candidate kinesins are displayed in Fig 3B. Of the eight kinesins selected by the screen KIF22, KIF14 and KIF13A were not tested for degradation as KIF22 was a known substrate (Feine *et al*, 2007) and KIF14 and KIF13A did not easily translate *in vitro* due to their molecular weights of ≥185 kDa. Although KIFC1 had been suggested to be regulated by ubiquitination during the cell cycle (Zhao *et al*, 2008), this protein has not been studied further in the context of APC/C degradation and thus was included in the degradation assays.

We then turned to the well established *in vitro* degradation assay using G1 HeLa cell extracts, which maintain high APC/C^{CDH1} activity in order to test whether this E3 complex targets KIF18A, KIF2C, KIF23, KIFC1 and KIF4A for degradation by the proteasome (Pe'er *et al*, 2013). We added two additional kinesins as negative controls: KIF20A at the 50th percentile and KLC1 at the 96th percentile (Fig 2). All seven kinesins were expressed in an *in vitro* transcription/translation system in the presence of ^{35}S-methionine and incubated in HeLa S3 G1-phase extracts – conditions under which SECURIN, a prototypic APC/C substrate, is readily degraded. Two inhibition controls were also used to confirm APC/C-specific degradation: (i) addition of the C-terminal domain of the APC/C-binding region of EMI1 as a non-competitive inhibitor and (ii) addition of an excess of recombinantly expressed and His-tag purified non-radioactive SECURIN as a competitive inhibitor (Fig 4A and Supplementary Fig S3A) (Ayad *et al*, 2005; Schmidt *et al*, 2006). If degradation of the substrate is observed in the presence of either inhibitor, it would indicate APC/C-independent degradation modulated by an alternative E3 ligase.

A

Kinesin	% C1	% C2	% C3	% C4	% C5	% C6	median
KIF18A	**0.004**	**0.003**	**0.002**	**0.008**	**0.001**	0.01	**0.004**
KIF22	0.047	0.011	**0.002**	**0.004**	0.026	**0.001**	**0.007**
KIF2C	0.015	**0.009**	**0.005**	**0.006**	0.015	**0.006**	**0.008**
KIF23	0.015	**0.005**	**0.003**	**0.001**	0.018	0.02	0.01
KIF14	0.124	0.018	**0.004**	**0.002**	0.127	**0.001**	0.011
KIFC1	**0.002**	**0.002**	0.032	0.032	**0.006**	0.623	0.019
KIF13A	0.066	0.045	0.029	0.022	0.077	0.042	0.044
KIF4A	0.031	0.038	0.06	0.078	0.03	0.179	0.049
KIF2A	0.086	0.083	0.078	0.128	0.053	0.085	0.084
KIF4B	0.028	0.09	0.312	0.507	0.024	0.568	0.201
KIF11	0.084	0.156	0.573	0.307	0.379	0.768	0.343
KIF16B	**0.003**	0.021	0.759	0.651	0.055	0.938	0.353
KIF5B	0.598	0.447	0.295	0.342	0.454	0.169	0.394
KIF7	0.445	0.324	0.409	0.283	0.586	0.611	0.427
KIF20A	0.377	0.266	0.614	0.092	0.797	0.807	0.496
KIF21A	0.902	0.913	0.941	0.951	0.906	0.954	0.927
KLC2	0.921	0.947	0.945	0.957	0.911	0.93	0.937
KIF5A	0.953	0.947	0.936	0.952	0.924	0.9	0.941
KIF5C	0.979	0.969	0.938	0.896	0.975	0.874	0.953
KLC1	0.914	0.957	0.972	0.972	0.943	0.976	0.965

B

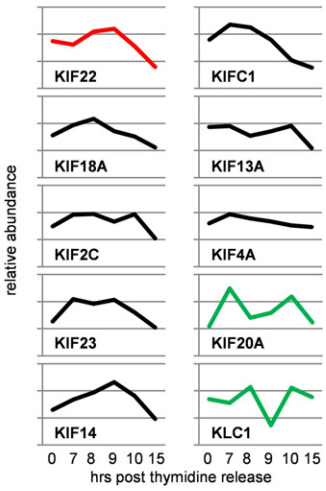

Figure 3. Co-regulation analysis reveals kinesins as putative novel APC/C targets.

A Heat map reflecting the percentile (%) in which the kinesins identified in our analysis are ranked in the six reference clusters (C1–C6). Boxed kinesins were flagged as putative APC/C targets based on their median percentile. Bolded values indicate ranks within the 1st percentile of each cluster.

B Individual protein abundance profiles for kinesins flagged as candidate (black traces) and non-candidate (green traces) APC/C substrates. KIF22, a known APC/C substrate, is indicated in red. The y-axes indicate relative abundance ranging from 0 to 0.3.

Our *in vitro* degradation assays showed a time-dependent degradation for four of the five potential substrates tested: KIF18A, KIF2C, KIFC1 and KIF4A were readily degraded *in vitro*, however remained stable in the presence of either APC/C inhibitor (Fig 4A and Supplementary Fig S3A). In contrast, inconclusive results were obtained for KIF23 and degradation was not observed for the two negative controls KIF20A and KLC1 under the conditions of our assay (Fig 4A and Supplementary Fig S3A).

APC/C substrates have two possible recognition motifs: the destruction box (D-box), and the KEN-box. However, neither motif is sufficient or necessary for degradation thereby making it challenging to develop sensitive and specific bioinformatics approaches for the *de novo* prediction of APC/C substrates. The D-box consensus sequence was initially characterized as RXXL (Glotzer *et al*, 1991; Pfleger & Kirschner, 2000). For follow-up experiments, we selected KIF18A and KIFC1 with 5 and 6 candidate D-box motifs, respectively, to verify which of their multiple RXXL motifs serve as the *bona fide* D-boxes. These kinesins represent two distinct classes of kinesins: KIF18A is a conventional kinesin with an N-terminal motor domain, followed by the coiled-coil stalk and the C-terminal head domain, and KIFC1 is one of three "inverted" kinesins with an N-terminal head-domain followed by the stalk and a C-terminal motor domain (Miki *et al*, 2005). Site-directed mutagenesis of each individual candidate D-box (RXXL → GXXV) revealed that mutation of a single motif close to the N-terminus (G5V8) rendered KIFC1 stable in G1 extracts with APC/C active, whereas either one of two RXXL mutations towards the C-terminus, G283V286 or G668V671, rendered KIF18A stable in the assay (Fig 4B).

Given that KIFC1 has an important role in spindle assembly and the bi-polar arrangement of mitotic microtubules (Walczak *et al*, 1997; Cai *et al*, 2009b), we further investigated the importance of APC/C-dependent degradation in the modulation of KIFC1 function during mitosis. To determine which of the APC/C co-activators, CDC20 or CDH1, regulate KIFC1 degradation, we used the *Xenopus laevis* egg extract system described in detail by Pe'er *et al* (Pe'er *et al*, 2013). This system allows the manipulation of the co-activator binding to the APC/C. APC/C^{CDC20} is highly active in interphase extracts that are driven into mitosis by adding an excess of non-degradable CYCLIN B1 (Lorca *et al*, 1998). Conversely, APC/C^{CDH1} activity can be introduced in interphase egg extracts by adding recombinant CDH1 which is not present in early embryos. Wild-type KIFC1 was assayed in both frog egg extracts featuring APC/C^{CDC20} and APC/C^{CDH1} activity, respectively, and was found to be degraded exclusively in extracts with APC/C^{CDH1}, but not in the extracts with APC/C^{CDC20} activity. Furthermore, when incubating the stabilized KIFC1 D-box mutant with APC/C^{CDH1} extract, no degradation could be observed (Supplementary Fig S3B). We followed up further by confirming, *in vitro*, that ubiquitination of WT-KIFC1 by the APC/C was reduced when the D-box mutation was introduced (Fig 4C).

It is not clear which cellular cues promote ubiquitination of a particular substrate by the APC/C. However, previous studies have demonstrated that phosphorylation dynamics can play a role in the susceptibility of an APC/C substrate for degradation (Littlepage *et al*, 2002; Holt *et al*, 2008). We used FLEXIQuant, a quantitative proteomics strategy developed by our group (Singh *et al*, 2009, 2012b), to conduct a more detailed quantitative characterization of KIFC1 and its cell cycle-dependent PTM patterns. We therefore *in vitro* synthesized an isotopically labeled variant of KIFC1 to serve as an internal standard for quantitative MS. The relative peak profiles of the endogenous (light) KIFC1 peptides versus their respective *in vitro* labeled (heavy) variants inform us about the relative stoichiometries of each observed KIFC1 peptide throughout the cell cycle. Lower than expected endogenous-to-heavy labeled peptide ratios are hallmarks for post-translational events.

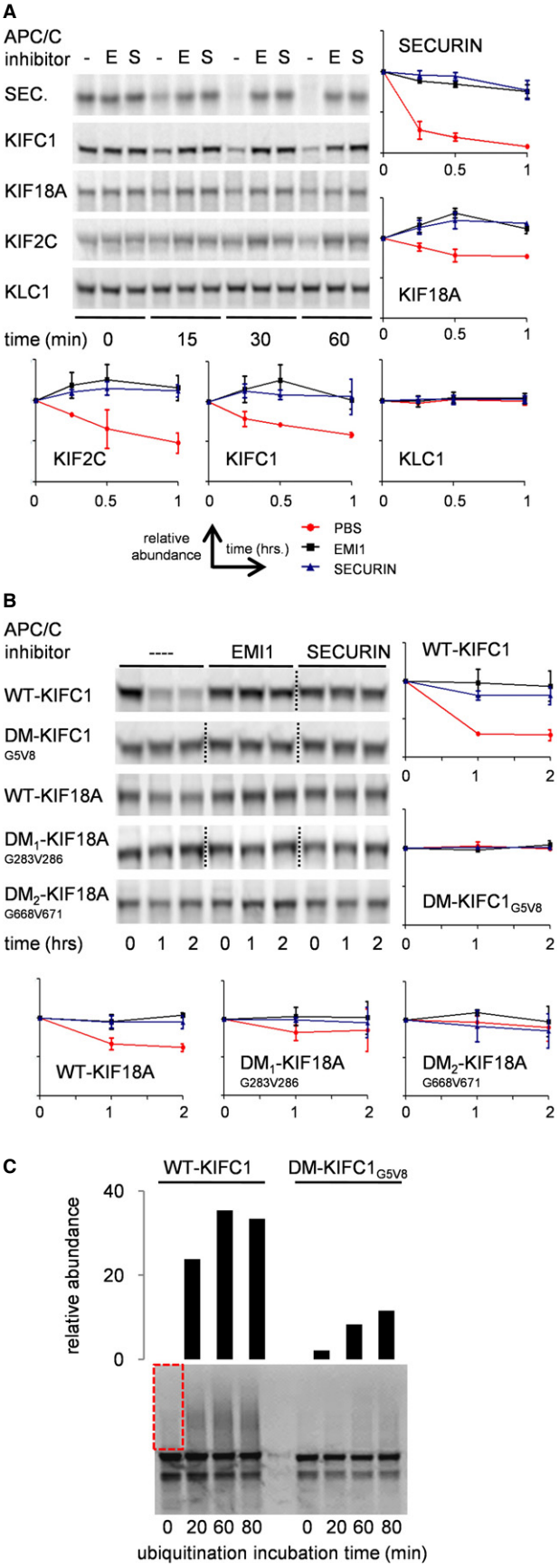

Figure 4. ***In vitro*** **APC/C-dependent degradation assays on selected kinesins.**

A Results of the degradation assays of ^{35}S-labeled kinesins KIFC1, KIF18A and KIF2C as a function of incubation with G1, i.e. APC/C^{CDH1}-active, HeLa S3 cell extracts in the presence or absence of the APC/C inhibitors EMI1 and SECURIN. The known APC/C substrate SECURIN and kinesin light chain 1 (KLC1) serve as a positive and negative control, respectively. The densitometry-based quantification results of three independent degradation assays are shown.

B Results of the degradation assays of ^{35}S-labeled WT or D-box mutants (DM) of KIFC1, KIF18A and SECURIN (positive control) in G1 cell extracts in the presence or absence of the APC/C inhibitors EMI1 and SECURIN. The densitometry-based quantification results of three independent degradation assays are shown. Of note: all lanes for each individual construct come from the same gel, but empty/irrelevant lanes were removed for clarity. The former location of these irrelevant lanes are indicated by dotted black lines; please see accompanying Source Data for scans of the complete gel images.

C APC/C-dependent *in vitro* ubiquitination of either ^{35}S-labeled WT or D-box mutated KIFC1. The high-molecular-weight smearing in the gel indicates ubiquitinated ^{35}S-KIFC1 (the red box indicates the quantified area). The poly-ubiquitinated forms of WT and mutant KIFC1 were quantified and normalized to the 0 h time point.

Source data are available online for this figure.

Using our unbiased FLEXIQuant approach, we analyzed similar time points used for the quantitative proteomics screen to identify peptides that show dynamic PTMs coinciding with APC/C activity. The FLEXIQuant analysis of KIFC1 resulted in approximately 50% sequence coverage (Fig 5A) across various biological repeats using different synchronization and immunoprecipitation (IP) protocols. The results of the normalized light-to-heavy abundance ratios for all observed peptides in each IP experiment are shown in Fig 5B. Two independent IPs show a clear cell cycle-dependent loss in intensity for a single endogenous peptide (Fig 5B, solid red trace), with the greatest decrease in signal intensity coinciding with mitosis and full recovery upon entry into G1 phase, an abundance profile correlating with APC/C activity. The maximum extent of this peptide signal loss during the time-course experiment was approximately 40% for the thymidine arrest-based synchronization (Fig 5B and C), and approximately 85% for the thymidine/nocodazole-based synchronization (data not shown), indicating an equivalent modification stoichiometry, respectively. This cell cycle-dependent abundance profile could be assigned in these FLEXIQuant experiments to the tryptic peptide S_6PLLEVK$_{12}$ (Supplementary Fig S4A). Interestingly, this particular peptide contains part of KIFC1's D-box motif. Considering the sequence of this peptide, the most likely PTM is a phosphorylation at Ser6, which is also conserved across numerous species (Supplementary Fig S4B). Furthermore, the phosphorylation of this Ser6 site has been described before in several phosphoproteomics studies (Malik *et al*, 2009; Olsen *et al*, 2010; Wang *et al*, 2010). Further analysis of the FLEXIQuant data identified Ser6, Ser26 and Ser31 as being phosphorylated (example MS/MS spectra shown in Supplementary Fig S4A, C and D); all sites have been described previously (Dephoure *et al*, 2008; Olsen *et al*, 2010). In contrast to the Ser6-containing peptide, which showed a clear cell cycle-dependent dynamics, no such cell cycle dependence was observed for the Ser26- and Ser31-containing peptide (Fig 5B and C, dashed red trace).

Given the cell cycle dependence and the extent of the Ser6 phosphorylation site, we hypothesized that this phosphorylation

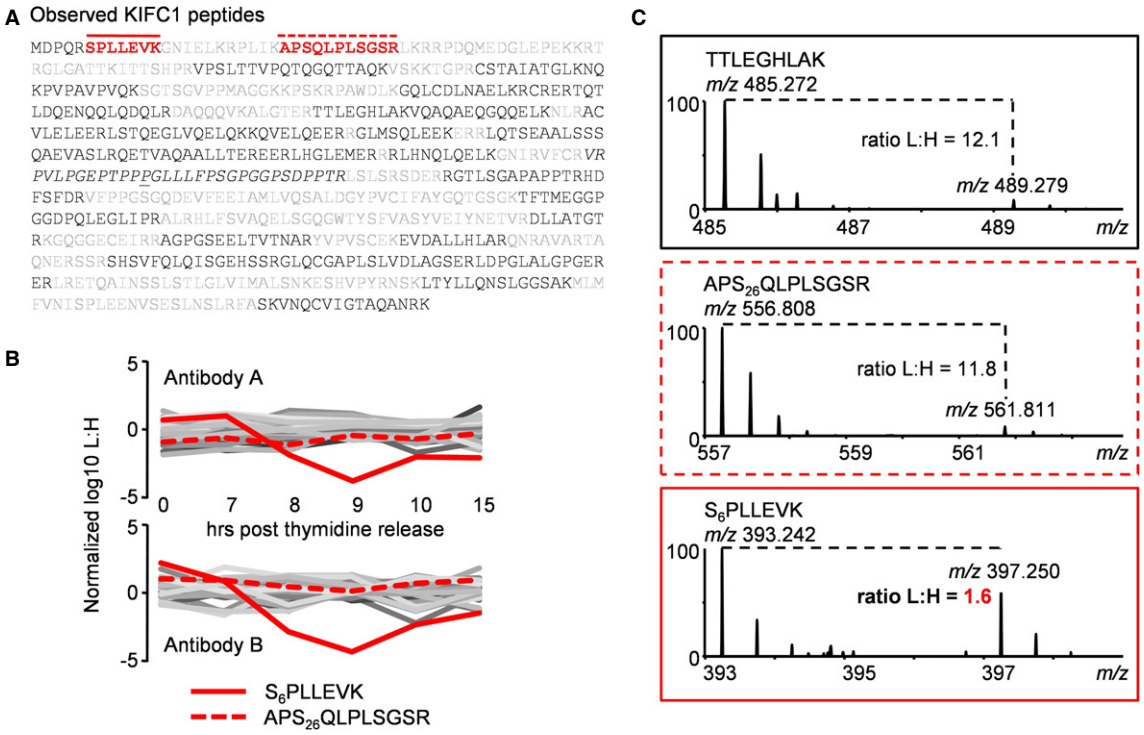

Figure 5. Identification and quantification of a cell cycle-dependent phosphorylation site in KIFC1.

A Observed sequence coverage for KIFC1. Sequence stretches in grey were not observed. Sequences indicated in red pertain to the corresponding traces in (B). The FLEXIQuant KIFC1 clone contained an amino acid variant (T368P, italicized tryptic peptide) (Gerhard *et al*, 2004); this peptide was not used for further analysis.

B FLEXIQuant analysis of normalized KIFC1 peptide abundances across the cell cycle. Two different antibodies (A: SIGMA or B: Bethyl Laboratories) were used for immunoprecipitating KIFC1. The red, solid trace highlights the peptide that is post-translationally modified during mitosis to a significant extent (corresponding to phosphopeptide containing pS6). The red, dashed trace highlights the peptide with the known phosphorylation sites S26 or S31 that is not modified in a cell cycle-dependent manner.

C Three FLEXIQuant-based KIFC1-derived peptide peak pairs as observed in the sample collected 9 hours post thymidine release: Two peptides (TTLEGHLAK and APSQLPLSGSR) are not significantly modified and thus do not show a deviation from the mean (L:H = 12.4). In contrast, the peptide SPLLEVK is modified to a considerable extent showing a significant deviation from the mean (L:H = 1.6 versus 12.4). The red dashed and solid frames correspond to the peptide trace profiles in (B).

within the KIFC1 D-box motif could protect KIFC1 from premature degradation by the APC/C; a similar effect has been described for phosphorylation sites close to the degradation motifs of AURORA kinase A (AURKA) (Littlepage & Ruderman, 2002) and SECURIN (Holt *et al*, 2008). Such phosphorylation-dependent inhibition of the APC/C-dependent degradation can sharpen the switch between different phases as reported for SECURIN (Holt *et al*, 2008), and i.e. act to negatively regulate degradation by the APC/C until necessary (Littlepage *et al*, 2002; Crane *et al*, 2004a). Alternatively (and not mutually exclusive), such a phosphorylation can be a means of ensuring the proper ordering of the APC/C-dependent degradation of (a subset of) the various APC/C substrates. To test the latter hypotheses, we mutated Ser6 to either an alanine or an aspartate residue to mimic loss of phosphorylation or constitutive phosphorylation, respectively, and tested the effect of these mutations on the APC/C-dependent degradation of KIFC1 using *in vitro* degradation assays as described above. As functional controls, we also mutated the other two N-terminal phosphorylation sites Ser26 and Ser31 to alanine or aspartate. Additional positive and negative controls included wild-type KIFC1 and its D-box mutant.

The only phosphorylation site mutation that rendered KIFC1 resistant to degradation similar to the D-box mutant was the Ser6 to Asp substitution (S6D), mimicking constitutive phosphorylation. All other mutations showed the same APC/C-dependent degradation as the wild-type KIFC1 (Fig 6A and Supplementary Fig S5A). Although Ser6 is located within the active D-box, its mutation does not affect the functionality of the D-box as demonstrated by the unaltered APC/C-dependent degradation of the S6A mutant. The degradation of this S6A mutant clearly shows that Ser6 is not part of the D-box function itself, but has a unique and distinct role in the phosphorylation-induced degradation inhibition mechanism.

Ser6 is followed by a Pro residue. This well-known SP-motif led to the hypothesis that CDK1/CYCLIN B is the relevant kinase responsible for the cell cycle-dependent phosphorylation and stabilization of KIFC1, similar to what has been described for SECURIN (Holt *et al*, 2008). To test this hypothesis, we carried out *in vitro* phosphorylation assays with KIFC1 in the presence of CDK1/CYCLIN B. Tryptic digests of KIFC1 treated with CDK1/CYCLIN B were analyzed by LC-MS/MS revealing phosphorylation at Ser6 (Supplementary Fig S5B). To verify that this phosphorylation event could indeed impact the ubiquitination of KIFC1, *in vitro*

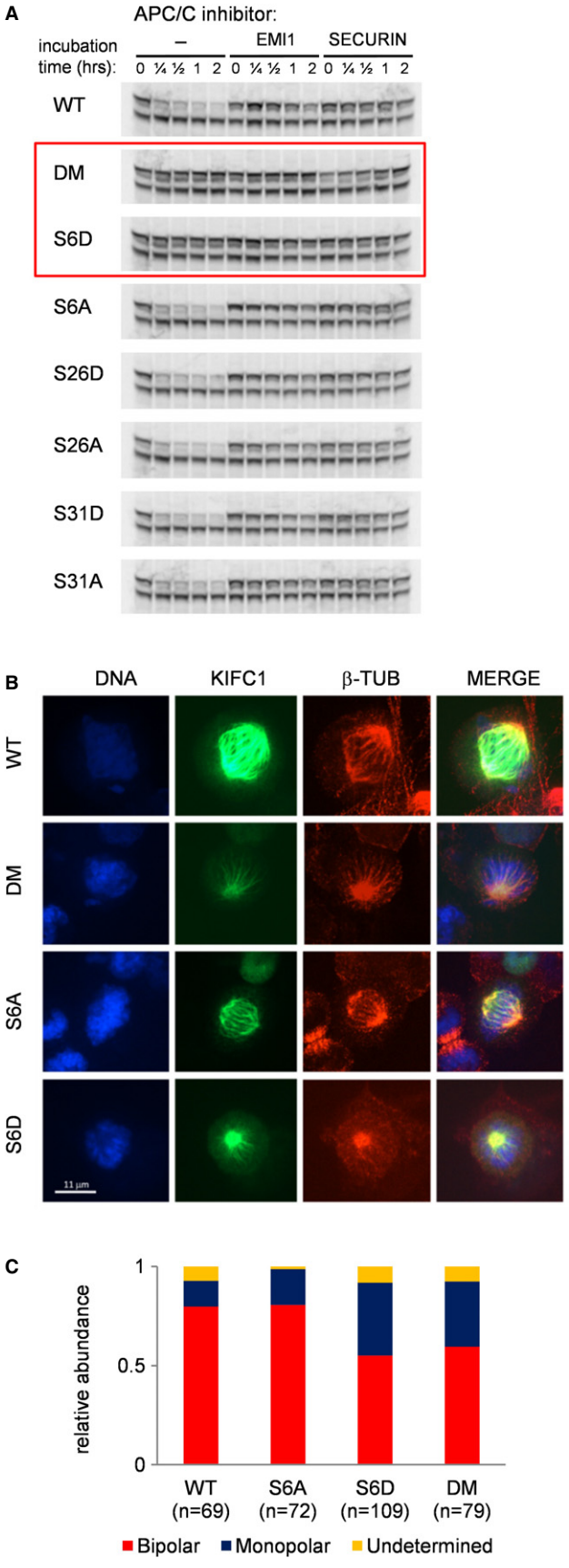

Figure 6. Functional analysis of the Ser6 phosphorylations.

A Degradation assays of ^{35}S-labeled WT-KIFC1, DM-KIFC1, and various serine-to-alanine and serine-to-aspartic acid mutants in G1 cell extracts in the absence/presence of recombinant EMI1 and SECURIN. Red box indicates mutants (DM and S6D) that are resistant to APC/C-dependent degradation.

B Non-degradable KIFC1 induces the monopolar spindle phenotype in mitotic cells. HeLa cells expressing WT or mutant KIFC1-tagged with eGFP were fixed 36 h post transfection, and labeled with DAPI (DNA) and anti-β-TUBULIN antibodies. Representative images from the normal bipolar (WT, S6A) and abnormal monopolar (DM, S6D) phenotypes are shown.

C The fraction of bipolar and monopolar spindle cells, 36 h post transfection with the depicted expression constructs.

Source data are available online for this figure.

ubiquitination assays of ^{35}S-KIFC1 were conducted either post treatment with CDK1/CYCLIN B or post treatment with CDK1/CYCLIN B co-incubated with Purvalanol A, a known CDK1 inhibitor (Villerbu *et al*, 2002). Treatment with the kinase alone reduced ubiquitination levels of KIFC1, whereas inhibition of CDK1 in a similar treatment resulted in ubiquitination to a similar extent as the unphosphorylated protein (Supplementary Fig S5C). These data indicate that phosphorylation by CDK1/CYLCIN B contributes to KIFC1 stability by protecting KIFC1 from APC/C-mediated ubiquitination and subsequent proteasomal degradation.

Next, we tested the implications of stabilizing KIFC1. Given that the motor forces exerted by minus end-directed KIFC1 on microtubules counterbalance the plus end-directed Eg5/KIF11 forces, we hypothesized that stabilization of KIFC1 might affect the microtubule dynamics due to the resulting imbalances of the KIFC1-Eg5 equilibrium. To test this hypothesis, we transfected HeLa S3 cells with GFP-labeled versions of either the wild-type, D-box, S6D or S6A KIFC1; all constructs were C-terminally tagged with GFP in order to minimize any influence on the N-terminal D-box (Crane *et al*, 2004b). Since overexpression assays need to be carefully interpreted, we used wild-type KIFC1 overexpression as our control and all phenotypes were scored relative to wild-type KIFC1 overexpression.

The overexpression of wild-type KIFC1 was sufficient to induce a monopolar spindle phenotype in approximately 15% of all mitotic cells (marked by a condensed chromatin structure as visualized with DAPI staining). Similar percentages were observed when overexpressing the non-stabilized KIFC1 S6A mutant (Fig 6B and C). In contrast, transfection of either the stabilizing D-box or S6D KIFC1 mutant increased the propensity of the monopolar spindle phenotype to 30–40% of the total mitotic cells analyzed (Fig 6B and C).

Discussion

In this study we employed our previously published protein profile similarity screening strategy (Kirchner *et al*, 2010) to identify putative APC/C substrates from a quantitative global proteomics dataset that profiles 4,470 proteins as a function of the cell cycle. In contrast to alternative substrate screening strategies that rely on *in vitro* conditions or focus on ubiquitination in general (Merbl & Kirschner, 2009; Kim *et al*, 2011; Wagner *et al*, 2011) our approach evaluates

the biologically relevant *in vivo* protein degradation as a function of the cell cycle. Candidate proteins are systematically evaluated, based on their protein profiles and selected for validation studies. Our hypothesis was that the mitotic abundance profiles of yet unknown APC/C substrates will resemble those of the quantified known APC/C substrates identified in our study (Fig 2). As such, we monitored protein profiles across mitosis using the tandem mass tag (TMT) strategy which permitted the simultaneous analysis of six cell cycle stages before, during and after mitosis (Fig 1). Using the abundance profiles of the identified known APC/C substrates as references we performed co-regulation analysis using our protein profile similarity screening strategy to identify other proteins with similar abundance profiles. The top 1% of proteins from the protein profile similarity screen showed an 18-fold enrichment of kinesins (Fig 3A) which led us to investigate whether kinesins are more commonly degraded in an APC/C dependent manner than previously thought.

Kinesins are microtubule-associated motor proteins, some of which are known to regulate microtubule dynamics during cell division. As such, some kinesins have been described as potential targets for cancer drug development. For example, small molecule inhibitors of the kinesins KIF11 (EG5) and KIF10 (CENPE) are both in clinical trials as cancer therapies (Rath & Kozielski, 2012). Considering the massive rearrangement of the microtubule cytoskeleton and chromosomes during mitosis, it is surprising that only two yeast kinesins, KIP1 and CIN8, and two human kinesins, KIF18A and KIF22, have been identified as APC/C substrates thus far (Gordon & Roof, 2001; Hildebrandt & Hoyt, 2001; Feine *et al*, 2007; Sedgwick *et al*, 2013).

Given that several kinesins showed such tight co-regulation in a large-scale experiment where more than 4,400 proteins were profiled across mitosis and that these proteins could be potential targets for anti-cancer drugs, we tested whether these candidate proteins were indeed *bona fide* APC/C substrates. We used the well-established biochemical *in vitro* degradation assay to validate the short list of potential APC/C targets. Four of five tested candidate kinesins, KIFC1, KIF18A, KIF2C, and KIF4A exhibited APC/C-dependent degradation profiles in our assay system (Fig 4A, and Supplementary Fig S3A). KIF23 resulted in inconclusive degradation profiles under the applied assay conditions (Supplementary Fig S3A).

We then focused on understanding the mechanisms behind APC/C-mediated degradation of KIFC1 and KIF18A. These two kinesins both play clear but distinct roles in cell division. For instance, KIFC1 and its opposing motor KIF11/EG5 are involved in organizing microtubule spindle structure observed in mitosis. First, we identified their D-box motifs: one was identified at the N-terminus of KIFC1 and two were identified within the C-terminal half of KIF18A. Interestingly, during the course of this work, Liu *et al* (2012) published an *in silico* study aimed at computationally screening for APC/C substrates based on D-box and KEN-box motifs. This study predicted that a number of kinesins are candidate APC/C substrates with KIFC1 and KIF4A as predicted D-box dependent substrates and KIF18A, KIF23 and KIF14A as KEN-box dependent substrates. We confirmed that the R_5SPL_8 sequence of KIFC1 is indeed a D-box motif. After successfully identifying the relevant D-boxes, we did not investigate any putative KEN-box motifs. However, it is now apparent that a given substrate can be APC/C-regulated by multiple recognition sites as demonstrated previously (Crane *et al*, 2004b), and recently by an excellent structural-guided biochemical study (Tian *et al*, 2012). KIF18A for example appears to possess at least two D-box motifs necessary for degradation based on our experiments, in addition to the predicted tentative KEN box (Liu *et al*, 2012). The biological relevance of possessing multiple recognition sites has not been fully investigated in the field in general and is beyond the scope of this study. It is nonetheless plausible that multiple sites may generate a kinetic proofreading mechanism that regulates the susceptibility and timing of degradation.

A number of studies have investigated the roles and mechanisms by which KIFC1 regulates bi-polarization of mitotic spindles (Mountain *et al*, 1999; Cai *et al*, 2009a,b), however, none have made a direct link between timely degradation by the APC/C and the function of KIFC1 during mitosis. First, we established that KIFC1 is a CDH1-specific target (Supplementary Fig S4C), suggesting that KIFC1 degradation occurs later in mitosis or early in G1 as is the case for a number of CDH1 targets. APC/C substrates are degraded in a very precisely ordered fashion to ensure the fidelity of cell division (Peters, 2006). We hypothesized that PTMs are involved in fine-tuning this timing precision. We tested this hypothesis of cell cycle-dependent PTMs using our recently developed FLEXIQuant approach which allows for an unbiased identification of peptides that harbor PTM(s) and the quantification of the extent of the PTM (Singh *et al*, 2009, 2012b). One specific advantage of this method is that it prioritizes potential PTM sites for subsequent follow-up experiments. While the standard qualitative MS data revealed three KIFC1 phosphorylation sites on Ser6, Ser26 and Ser31, FLEXIQuant demonstrated that only the abundance profile of the unmodified peptide $S_6PLLEVK_{12}$ is clearly modulated during the transition through mitosis, whereas the peptide harboring Ser26 and Ser31 demonstrated negligible changes during mitosis indicating low mitosis dependency of these two phosphorylation sites (Fig 5B). Given the timing of phosphorylation and placement of Ser6 within the D-box motif, a clearer picture emerged when considering two previous studies that demonstrated the role for specific phosphorylation sites in protecting the respective protein from APC/C-mediated degradation (Holt *et al*, 2008; Cai *et al*, 2009b). In each study, a phosphorylation site proximal to confirmed APC/C recognition motifs rendered their given substrates, SECURIN and AURORA A, resistant to degradation. In the case of KIFC1, however, the stabilizing phosphorylation site is located within the D-box itself.

Site-directed mutagenesis of three identified phosphorylation sites was performed. Only the S6D mutation could stabilize KIFC1 levels whereas all other serine mutants displayed normal degradation profiles similar to the wild-type (Fig 6A and Supplementary Fig S5A). Overall these findings are consistent with the growing notion that phosphorylation at specific sites within a substrate play a crucial role in preventing premature recognition and ubiquitination by the APC/C and hence the general timing of events in mitosis (Littlepage *et al*, 2002; Holt *et al*, 2008). We and others (Ozlu *et al*, 2010; Kettenbach *et al*, 2011) have shown that CDK1 plays a major role in mitosis and thus may be the kinase involved in stabilization of KIFC1. We confirmed that CDK1 phosphorylates Ser6 (Supplementary Fig S5B) and demonstrated that KIFC1 displays CDK1-mediated resistance to ubiquitination by the APC/C (Fig S5C). Thus, the mechanism that mediates KIFC1 and APC/C interactions must also account for the roles of the mitotic phosphatases. The precise phosphatase(s) responsible for dephosphorylation of Ser6 have yet to be

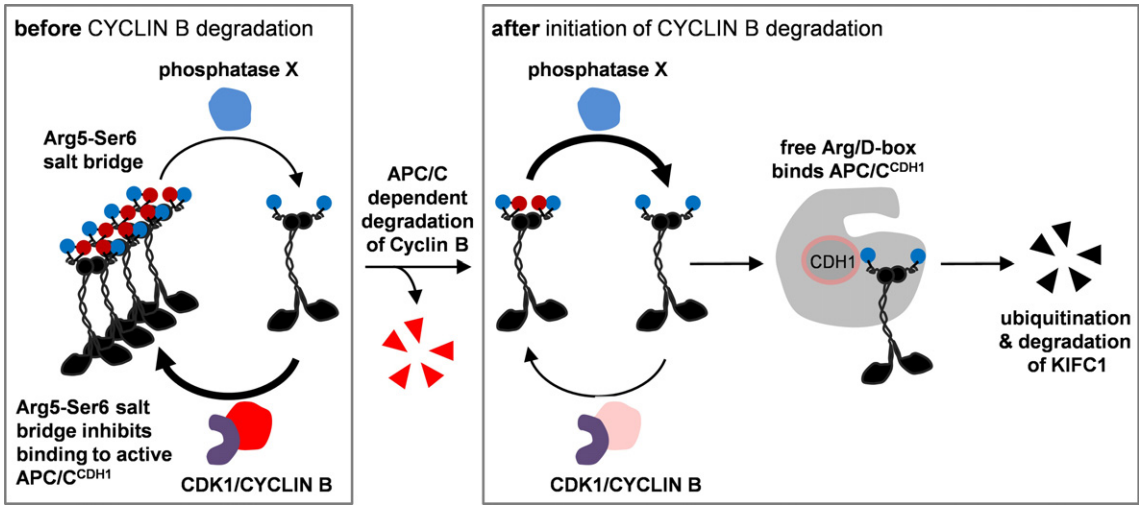

Figure 7. Model for phosphorylation-dependent inhibition of APC/C-mediated degradation of KIFC1.
Phosphorylation of KIFC1 at Ser6 by CDK1 renders KIFC1 incapable of binding to the APC/C^{CDH1}. The phosphate may form a salt bridge with the neighboring arginine which is a key residue in the APC/C recognition motif, the D-box. Removal of the phosphorylation by a phosphatase permits APC/C access to the D-box for subsequent ubiquitination and degradation.

identified, but can be postulated as PP2A (Wurzenberger & Gerlich, 2011).

Overexpression of wild-type KIFC1 in cells disturbs the stoichiometric balance between KIFC1 and its counterforce generating kinesin EG5/KIF11. This imbalance may be responsible for the increased number of monopolar spindles observed. However, this phenotype was even more profound in cells overexpressing non-degradable D-box or S6D of KIFC1 (Fig 6C), which was not observed with other phosphorylation site mutants. We consider these results as consistent with the notion that the down-regulation of the KIFC1 antagonist EG5/KIF11 induces a monopolar spindle phenotype and that the decrease of KIFC1 by RNA interference can induce multipolar spindles (Zhu *et al*, 2005). However, it remains an unanswered question as to how degradation late in mitosis will show an effect early in the following mitosis as CDH1 knockdown experiments did not show any defects in early spindle formation (Floyd *et al*, 2008). More detailed experiments are required to answer this question.

Our model in Fig 7 summarizes our findings in the context of previous structural studies of the APC/C (da Fonseca *et al*, 2011; He *et al*, 2013). It proposes that KIFC1 susceptibility to the APC/C is in part controlled by phosphorylation at Ser6. For example, a CDK1-dependent phosphorylation at Ser6 may result in a salt bridge with Arg5, preventing Arg5 of the D-box to bind to the APC/C. However, other models of modulating the interaction between the APC/C and KIFC1 are possible. Recent structural data of the C-terminal WD40 domain of *S. cerevisiae* CDH1 in complex with the APC/C inhibitor, Acm1, reveal hydrogen bond interactions between the D-box arginine of Acm1, and two acidic residues (glutamate and aspartate) from CDH1 (He *et al*, 2013), which is consistent with the model of phosphorylation inhibition proposed above. While this structural study provides some insight into the structural underpinnings of the observed phenotypes of our KIFC1 mutants, only more in-depth structure-guided mutational analysis can test the precise mechanism behind the KIFC1 D-box phosphorylation and binding to the APC/C.

The timely degradation of substrates is imperative for the fidelity of mitosis and Rape *et al* have showed that substrate ordering depends on the relative processivity of substrate multi-ubiquitination by the APC/C which is strongly influenced by the D-box (Rape *et al*, 2006). This study suggested that earlier substrates are better substrates of the APC/C. Our study and others (Littlepage & Ruderman, 2002; Holt *et al*, 2008) suggest that PTMs such as phosphorylation fine tune the degradation of these substrates further to ensure the temporal order of degradation. Overall, both published and presented data from this study are consistent with the emerging model that coordinated stabilization and degradation of several mitotic kinesins in general is important for proper mitosis. The timely degradation of kinesins and many other substrates is probably tightly regulated by PTMs as observed with KIFC1. As the kinesins are major regulators of cytoskeleton reorganization during mitosis, our study emphasizes the role of APC/C coordinating cytoskeleton topology in the context of cell division.

Materials and Methods

Cell culture

Reagents were purchased from Sigma-Aldrich unless otherwise noted. HeLa S3 cells (ATCC) were maintained in DMEM supplemented with 10% fetal bovine serum, penicillin and streptomycin (Cellgro).

For the mitosis TMT experiment, HeLa S3 cells were grown in 15-cm culture dishes until confluent, split in a 1-to-6 ratio and grown for 12 h. Cells were then incubated with 2 mM thymidine for 20–22 h, washed and released into fresh media for 8 h, incubated again with 2 mM thymidine for 20–22 h, and washed and released for up to 15 h. The time points sampled for the TMT labeling included, 0 h/S-phase (immediately before the second thymidine release), and 7, 8, 9, 10 and 15 h post-thymidine release.

For KIFC1 immunoprecipitation assays, S3 cells were synchronized as described for the mitosis TMT experiment. Cells were harvested at S-phase, and 4, 7, 8, 12 and 13 h post-thymidine release. For *in vitro* degradation assays, S3 cells were grown in suspension until the population reached a density of 2.5–3 × 10^5 cells/ml. Cells were then incubated with 2 mM thymidine for 20–22 h, washed and released into fresh media for 3 h, and blocked again with 0.1 μg/ml nocodazole for 11 h. Cells were washed twice with fresh warm media, released for 4 h and then harvested to obtain a G1 population. Synchronization for all experiments was validated using Flow Cytometry (5-laser LSRII; BD Biosciences) after propidium iodide staining of ethanol-fixed cells.

In vitro degradation, ubiquitination and kinase assays

Degradation assays - Extracts of HeLa S3 cells were prepared as described previously (Ayad *et al*, 2003). Degradation assays were done in 20-μl cell extracts supplemented with 1 μl of energy regenerating mix (20 mM ATP, 150 mM creatine phosphate, 2 mM EGTA pH 8.0, 20 mM MgCl2, 0.1 μg/ml Ubiquitin (Boston Biochem), 0.1 μg/ml Cyclohexamide), 1 μl of 1 mg/ml recombinant His6-UBE2S (Boston Biochem), 1 μl of 1 mg/ml recombinant UBCH10 (Boston Biochem), and either 5 μl of 0.5 mg/ml 6 × His-tag purified recombinant EMI1 (C-terminus) protein or SECURIN protein or PBS for no inhibitor control and 1–2 μl radiolabelled *in vitro* synthesized substrate expressed in reticulocyte lysate (Promega) with ^{35}S-labeled methionine. Ubiquitination assays were done by pulling down the APC/C (Singh *et al*, 2009), maintaining the complex on the beads, and supplementing the APC/C with recombinant CDH1 (Ayad *et al*, 2003) and reagents described above. Samples were incubated at 30°C and aliquots were sampled every 15–30 min over a 2-h period. Aliquots were added to Laemmli sample buffer (Bio-Rad), incubated at 95°C for 5 min, and flash-frozen on dry ice. Samples were resolved by SDS–PAGE and visualized by autoradiography. For kinase-ubiquitination assays, ^{35}S-labeled KIFC1 was pre-incubated with CDK1/CYCLIN B (plus or minus Purvalanol A) for 1 h at 30°C, and then added to the ubiquitination assay described above. To map phosphorylation sites due to incubation with CDK1/CYCLIN B, Ni-NTA-bound (GE Healthcare) His6-KIFC1 was incubated with CDK1/CYCLIN B for 3 h, and the sample processed for MS analysis as described in the below.

In order to obtain *X. laevis* egg extracts with interphase activities, frogs were injected with human chorionic gonadotropin, and laid eggs were collected and washed in 1X MMR prior to dejellying in 2% aqueous cysteine and activation with 1 μg/ml calcium ionophore (Sigma-Aldrich) (Pe'er et al, 2013). Next, the eggs were washed in XB buffer and XB buffer with protease inhibitor mix (Roche). Forty-five minutes post-activation, eggs were packed by centrifugation (1 min at 157 × *g*) in an Ultraclear centrifuge tube (Beckman Coulter, Inc.), supplemented with cytochalasin B (Sigma-Aldrich) and finally crushed by centrifugation (10 min at 15,680 × *g*). The cytoplasmic/top layer was collected and clarified by additional centrifugation (10 min at 15,680 × g). The following reagents were then added to the listed final concentrations eqivalent to 1X energy mix: 4% glycerol, 10 μg/ml cytochalasin B, and 100 μg/ml cycloheximide (Sigma-Aldrich). Protein degradation was assayed in interphase egg extracts in the presence or absence of 1 nM recombinant CDH1, or in extracts that were driven into mitosis by preincubation with 10 μg/ml Δ90 cyclin B1 for 40 min at room temperature. Irrespective of the extract, 1 μl ^{35}S-labeled protein substrate was mixed with 15 μl extracts, 1 μl of 20 × energy-regeneration mix, and 1 μl of 10 mg/ml ubiquitin. The reactions were incubated at room temperature for up to 2 h whereby aliquots were taken at the time points indicated in Supplementary Fig S3B, and processed for SDS-PAGE and autoradiography.

Plasmids

Human clones of KIFC1, KIF2C, KIF18A, KIF14, KIF20A, KIF22, KIF23 and KLC1 were purchased from Open Biosystems (OB), the KIF4A clone was a gift from the T. Mitchison Lab. The genes were subcloned into the CellFree Sciences (CFS) vector, pEU-E01-MCS, for *in vitro* degradation assays. KIFC1 was cloned into the pCS2 vector, the pCS2-Cterminal EGFP vector (Rape & Kirschner, 2004), and the CFS-based N-terminal His tag FLEXIQuant vector (Singh *et al*, 2009) for *in vitro* degradation assays, *in vivo* imaging, and FLEXIQuant analysis, respectively. The various D-box and serine mutations were generated using QuikChange site-directed mutagenesis strategy (Stratagene).

KIFC1 immunoprecipitations for FLEXIQuant analysis

HeLa S3 cells harvested from a 15-cm culture dish were lysed in 200 μl lysis buffer [1X PBS, 0.1% Triton X-100, 1 mM orthovanadate, 10 mM NaF and protease inhibitor cocktail (Roche)]. The cells were kept on ice for 15 min and then lysed by three rounds of freeze/thaw (liquid N2/30°C) cycling, followed by ten passages through a 27G needle. Lysates were centrifuged at 20,000 × *g* on a standard refrigerated tabletop centrifuge. Beforehand, the antibody (Bethyl or SIGMA) was conjugated to AffiPrep Protein A sepharose beads (Bio-Rad) in binding buffer containing 50 mM TrisHCl pH 7.4, 1% NP40, 150 mM NaCl, 1 mM EDTA, 1 mM PMSF, 1 mM Na_3VO_4, 1 mM NaF, and phosphatase inhibitor cocktails 1 and 2. Each HeLa S3 supernatant was mixed with an appropriate volume of wheat germ extract expressing stable isotope labeled KIFC1 (Singh *et al*, 2009), and subsequently added to the antibody. The antibody-lysate samples were incubated for 3 h at 4°C. Bound protein was washed six times with 10× bead volume of wash buffer (binding buffer + 300 mM NaCl). The bound protein was precipitated for 5 min at 95°C in 100 μl of Laemmli sample buffer. The immunoprecipitates were analyzed by SDS-PAGE and a molecular weight window around the observed band for precipitated KIFC1 was excised and digested using trypsin.

Immunostaining and microscopy

HeLa adherent cells (ATCC) were grown on 3–4 coverslips/well, in a 6-well flat-bottom tissue culture plate (BD Falcon) and transfected using polyethylenimine (MW 25K, Polysciences). For each well of cells, 30 μl of 0.5 mg/ml polyethylenimine was dissolved in 300 μl of 150 mM NaCl and mixed with 1.0 μg plasmid dissolved in 300 μl of 150 mM NaCl for 20 min before adding to the cells. WT or mutant pCS2-KIFC1-EGFP plasmids were transfected for 24 h prior to methanol fixation (3 min at −20°C). Cells were blocked (0.15 M NaCl, 0.02 M TrisHCl pH 7.4, 2% BSA, 0.1% Triton X-100, 0.1%

sodium azide) and subsequently incubated with anti-β-tubulin primary antibody (Sigma-Aldrich) for 1 h followed by the Alexa Fluor 568 rabbit anti-mouse secondary antibody (Invitrogen) for 1 h, at room temperature. Cells were mounted in Aqua-Mount (Lerner Laboratories) and kept at 4°C. Microscopy was done using the Perkin Elmer Ultraview Vox microscope and the data were imaged using the Velocity Image Analysis Software (IDDRC Imaging Core at Boston Children's Hospital).

TMT labeling and peptide fractionation

Three biological replicates were performed for each cell cycle experiment. Cells were lysed and the proteins extracted as outlined previously (Winter & Steen, 2011), digested using trypsin (Promega), and labeled with the TMT 6-plex reagent (Thermo Scientific), combined and desalted using Oasis Hlb 1 cc columns (Waters). The desalted peptide samples were fractionated based on their isoelectric point in a range of pI 3–10 in 24 fractions using an OFFGEL fractionator (Agilent). The fractions were extracted, dried with a table top speed vacuum (Thermo Scientific), resuspended in 20 μl 5% acetonitrile 5% formic acid and analyzed by LC-MS/MS in triplicate (for details see below), resulting in nine replicates for each time point when considering all three biological repeats.

Mass spectrometry

Peptide samples were analyzed with the high-resolution/accuracy LTQ-Orbitrap mass spectrometer (Thermo Scientific, Classic model, resolution setting for survey scans: 30K for the TMT experiments and 60K for FLEXIQuant analyses) linked to a micro-autosampler and a nanoflow HPLC pump (2D nanoLC, Eksigent). The reverse phase columns were packed in-house using Magic C18 particles (5 μm, 200 Å; Michrom) and PicoTip Emitters (New Objective). Peptides were eluted with a 30 (FLEXIQuant) or 60 min (TMT) linear gradient from 95% A (water with 0.2% formic acid) 5% B (acetonitrile with 0.2% formic acid) to 65% A 35% B. The data were acquired in the data dependent mode, fragmenting the 6 most abundant peptide species. For the TMT analyses, peptides were fragmented in the PQD-mode (Bantscheff *et al*, 2008). For FLEXIQuant analyses, peptides were fragmented in the CID mode.

The proprietary Thermo Scientific raw files were converted into mgf files (Renard *et al*, 2009) and MS/MS data queried either against the IPI Human v.3.69 protein sequence database (TMT experiments), containing common contaminations and concatenated to its decoy version, or an in-house custom database, containing FLEX-tagged human KIFC1 (for the FLEXIQuant experiments), using MASCOT version 2.1 (Matrix Science). TMT peptides were searched with enzyme specificity trypsin, one missed cleavage site, propionamide (Cys) as a fixed modification; and TMT6plex (N-termini and Lys), oxidation (Met), deamidation (N), and Gln to pyroGlu (N-terminal Q) as variable modifications. Using the target-decoy approach, peptides were filtered at a false discovery rate of 1% and proteins assigned based on at least two unique peptide sequences using in house software. After peptide and protein identification, IPI accession numbers were converted to NCBI gene names in order to overcome isoform and redundancy issues encountered when using the IPI databases.

Quantitative MS analysis and protein profile similarity screening

Pre-clustering steps

Peptide-spectrum matched TMT ion intensities were extracted from the fragment ion spectra without applying MS- or MS/MS-based cut-offs. Prior to further data analysis we corrected for loading variation. Next, each TMT ion channel intensity was divided by the sum of all sister channel intensities (sum normalization), which resulted in the peptide abundance profiles. As it has been recently shown that the Model-Based clustering based on finite mixture models (Banfield & Raftery, 1993; Fraley & Raftery, 2002) can be successfully applied to time series data analysis (Fröhwirth-Schnatter & Kaufmann, 2008) such that each time series y_i, i = 1,…,N, in a panel of N time points is considered to be a single entity connected by a line (Fig 1E–G). The protein abundance profile was calculated based on the average TMT–based peptide abundance profiles from all associated peptide-spectrum matches. Compositional data analysis was used in order to perform relative protein profiling (Aitchison, 1982, 1986). Compositional data consist of vectors whose components are the proportions of a whole (here set to be 1). Thus, the final sum normalized intensities calculated above provide the compositional vectors which correspond to the relative magnitudes of the reporter ions. The isometric log-ratio transform was subsequently applied enabling the use of the Euclidean distance metric for the compositional vectors (van den Boogaart & Tolosana-Delgado, 2008) for the clustering, protein profiling and co-regulation analysis.

Clustering steps

The profiles of the APC/C substrates identified in our screen were extracted and co-clustered using a Gaussian mixture model (Fraley & Raftery, 2002) in the simplicial domain. One of the advantages of this method is that the cluster analysis is based on probability models which permit an unbiased approach for determining potential APC/C target sub-clusters. The workflow of this algorithm (implemented in R as "Mclust") (Fraley *et al*, 2012) combines hierarchical agglomeration (Murtag & Raftery, 1984), (Banfield & Raftery, 1993), Expectation Maximization (EM) algorithm (McLachlan & Basford, 1988), with a Bayesian Information Criteria (BIC) approximation (Swartz, 1978). The overall complexity of the mixture model is governed by the degrees of freedom permitted by structure of the covariance matrices $\sum_k$ of the k clusters (Fraley *et al*, 2012). The best model minimizes the BIC (Swartz, 1978; Fraley *et al*, 2012): it delivers the best possible tradeoff between the number of clusters and the intra-cluster variances. This procedure yielded our six reference groups (Fig 2B). We subsequently determined a representative average protein trace for each reference group and determined the similarity of each observed protein trace to these reference protein traces. Proteins were then ranked according to decreasing similarity for every reference group. For the subsequent text analysis, the descriptions of the 45 proteins most similar to each of the six different reference profiles (top percentile, i.e. 270 protein descriptions in total) were concatenated and submitted to http://textalyser.net/ for text analysis to determine the frequency of each word.

For FLEXIQuant experiments, the area under the selected ion chromatograms for each light and heavy monoisotopic peak was

determined using Xcalibur (Thermo Scientific). Details on the data and statistical analyses have been outlined in our previous publication (Singh *et al*, 2012a).

Supplementary information for this article is available online: http://emboj.embopress.org

Acknowledgements

This work was in part funded by grants from the German Academic Exchange Service (DW), a Feodor Lynen Research Fellowship from the Alexander von Humboldt Foundation (MK), the NIH (HS: R01GM094844; JAS: R01NS066973) and a Junior Faculty Career Development Award from Harvard Medical School (JAS), the Israeli Centers of Research Excellence (I-CORE), Gene Regulation in Complex Human Disease, Center No. 41/11 (AT), the Israel Cancer Association Grant 20120067 (AT), and the German––Israeli Foundation (GIF), No. 2294-2269.2/2011 (AT). The imaging was done in the IDDRC Imaging Core (P30HD18655). Flow Cytometry experiments were carried out at the Harvard Stem Cell Institute at Boston Childrens Hospital, a Center for Molecular Developmental Hematopoiesis (P30DK049216). We also would like to thank T. Mitchison for the KIF4 plasmid, P. Ricchiuto for assisting with the clustering analysis, and W. Timm for helping with the initial data analysis.

Author contributions

SAS carried out the cell biological follow-up studies and devised the experiments to study the role of the KIFC1 phosphorylation; DW devised and carried out all the quantitative proteomics experiments including the preparation of the synchronized samples; furthermore he carried out the initial degradation assays; MK devised and carried out the computational analysis of the quantitative proteomics data; RC subcloned and mutated the constructs, devised the optimization of and carried out the majority of the ubiquitination and degradation experiments of the kinesins; SA carried out the cell culture experiments for the cell biological follow up experiments; NO provided expert cell biology advice and assisted with the in-depth analysis of the data; AT provided expert advice, and devised and carried out the initial preliminary cell biological follow up experiments; JAS and HS conceptualized the idea of using multiplexed quantitative proteomics for the identification of APC/C substrates, and supervised the experiments. In addition, JAS and HS carried out the initial proof of concept experiments. The manuscript was written by SAS, DW, MK, AT, JAS and HS. All authors critically read and revised the manuscript.

Conflict of interest

The authors declare that they have no conflict of interest.

References

Aitchison J (1982) The statistical analysis of compositional data. *J R Stat Soc Series B* 44: 139 – 177

Aitchison J (1986) *The Statistical Analysis of Compositional Data. Monographs on Statistics and Applied Probabilty*. London, UK: Chapman & Hall Ltd

Ayad NG, Rankin S, Murakami M, Jebanathirajah J, Gygi S, Kirschner MW (2003) Tome-1, a trigger of mitotic entry, is degraded during G1 via the APC. *Cell* 113: 101 – 113

Ayad NG, Rankin S, Ooi D, Rape M, Kirschner MW (2005) Identification of ubiquitin ligase substrates by *in vitro* expression cloning. *Methods Enzymol* 399: 404 – 414

Banfield JD, Raftery AE (1993) Model-based Gaussian and non-Gaussian clustering. *Biometrics* 49: 803 – 821

Bantscheff M, Boesche M, Eberhard D, Matthieson T, Sweetman G, Kuster B (2008) Robust and sensitive iTRAQ quantification on an LTQ orbitrap mass spectrometer. *Mol Cell Proteomics* 7: 1702 – 1713

van den Boogaart KG, Tolosana-Delgado R (2008) compositions: a unified R package to analyze compositional data. *Comput Geosci* 34: 320 – 338

Brady SM, Orlando DA, Lee JY, Wang JY, Koch J, Dinneny JR, Mace D, Ohler U, Benfey PN (2007a) A high-resolution root spatiotemporal map reveals dominant expression patterns. *Science* 318: 801 – 806

Brady SM, Song S, Dhugga KS, Rafalski JA, Benfey PN (2007b) Combining expression and comparative evolutionary analysis. The COBRA gene family. *Plant Physiol* 143: 172 – 187

Cai S, O'Connell CB, Khodjakov A, Walczak CE (2009a) Chromosome congression in the absence of kinetochore fibres. *Nat Cell Biol* 11: 832 – 838

Cai S, Weaver LN, Ems-McClung SC, Walczak CE (2009b) Kinesin-14 family proteins HSET/XCTK2 control spindle length by cross-linking and sliding microtubules. *Mol Biol Cell* 20: 1348 – 1359

Clute P, Pines J (1999) Temporal and spatial control of cyclin B1 destruction in metaphase. *Nat Cell Biol* 1: 82 – 87

Crane R, Gadea B, Littlepage L, Wu H, Ruderman JV (2004a) Aurora A, meiosis and mitosis. *Biol Cell* 96: 215 – 229

Crane R, Kloepfer A, Ruderman JV (2004b) Requirements for the destruction of human Aurora-A. *J Cell Sci* 117: 5975 – 5983

Dayon L, Hainard A, Licker V, Turck N, Kuhn K, Hochstrasser DF, Burkhard PR, Sanchez JC (2008) Relative quantification of proteins in human cerebrospinal fluids by MS/MS using 6-plex isobaric tags. *Anal Chem* 80: 2921 – 2931

Dephoure N, Zhou C, Villen J, Beausoleil SA, Bakalarski CE, Elledge SJ, Gygi SP (2008) A quantitative atlas of mitotic phosphorylation. *Proc Natl Acad Sci USA* 105: 10762 – 10767

Draetta G, Luca F, Westendorf J, Brizuela L, Ruderman J, Beach D (1989) Cdc2 protein kinase is complexed with both cyclin A and B: evidence for proteolytic inactivation of MPF. *Cell* 56: 829 – 838

Feine O, Zur A, Mahbubani H, Brandeis M (2007) Human kid is degraded by the APC/C-Cdh1 but not by the APC/C-Cdc20. *Cell Cycle* 6: 2516 – 2523

Floyd S, Pines J, Lindon C (2008) APC/C Cdh1 targets aurora kinase to control reorganization of the mitotic spindle at anaphase. *Curr Biol* 18: 1649 – 1658

da Fonseca PC, Kong EH, Zhang Z, Schreiber A, Williams MA, Morris EP, Barford D (2011) Structures of APC/C(Cdh1) with substrates identify Cdh1 and Apc10 as the D-box co-receptor. *Nature* 470: 274 – 278

Fraley C, Raftery A (2002) Model-based clustering, discriminant analysis, and density estimation. *J Am Stat Assoc* 97: 611 – 631

Fraley C, Raftery A, Murphy B, Scrucca L (2012) *mclust Version 4 for R: Normal Mixture Modeling for Model-Based Clustering, Classification, and Density Estimation*. Seattle, WA: University of Washington

Fröhwirth-Schnatter S, Kaufmann S (2008) Model-based clustering of multiple time series. *J Bus Econ Stat* 26: 78 – 89

Gerhard DS, Wagner L, Feingold EA, Shenmen CM, Grouse LH, Schuler G, Klein SL, Old S, Rasooly R, Good P, Guyer M, Peck AM, Derge JG, Lipman D, Collins FS, Jang W, Sherry S, Feolo M, Misquitta L, Lee E *et al* (2004) The status, quality, and expansion of the NIH full-length cDNA project: the Mammalian Gene Collection (MGC). *Genome Res* 14: 2121 – 2127

Glotzer M, Murray AW, Kirschner MW (1991) Cyclin is degraded by the ubiquitin pathway. *Nature* 349: 132 – 138

Gordon DM, Roof DM (2001) Degradation of the kinesin Kip1p at anaphase onset is mediated by the anaphase-promoting complex and Cdc20p. *Proc Natl Acad Sci USA* 98: 12515 – 12520

Hadwiger JA, Wittenberg C, Richardson HE, de Barros Lopes M, Reed SI (1989) A family of cyclin homologs that control the G1 phase in yeast. *Proc Natl Acad Sci USA* 86: 6255 – 6259

Hagting A, Den Elzen N, Vodermaier HC, Waizenegger IC, Peters JM, Pines J (2002) Human securin proteolysis is controlled by the spindle checkpoint and reveals when the APC/C switches from activation by Cdc20 to Cdh1. *J Cell Biol* 157: 1125 – 1137

He J, Chao WC, Zhang Z, Yang J, Cronin N, Barford D (2013) Insights into degron recognition by APC/C coactivators from the structure of an Acm1-Cdh1 complex. *Mol Cell* 50: 649 – 660

Hildebrandt ER, Hoyt MA (2001) Cell cycle-dependent degradation of the Saccharomyces cerevisiae spindle motor Cin8p requires APC(Cdh1) and a bipartite destruction sequence. *Mol Biol Cell* 12: 3402 – 3416

Holt LJ, Krutchinsky AN, Morgan DO (2008) Positive feedback sharpens the anaphase switch. *Nature* 454: 353 – 357

Kettenbach AN, Schweppe DK, Faherty BK, Pechenick D, Pletnev AA, Gerber SA (2011) Quantitative phosphoproteomics identifies substrates and functional modules of Aurora and Polo-like kinase activities in mitotic cells. *Sci Signal* 4: rs5

Kim W, Bennett EJ, Huttlin EL, Guo A, Li J, Possemato A, Sowa ME, Rad R, Rush J, Comb MJ, Harper JW, Gygi SP (2011) Systematic and quantitative assessment of the ubiquitin-modified proteome. *Mol Cell* 44: 325 – 340

King RW, Deshaies RJ, Peters JM, Kirschner MW (1996) How proteolysis drives the cell cycle. *Science* 274: 1652 – 1659

King RW, Peters JM, Tugendreich S, Rolfe M, Hieter P, Kirschner MW (1995) A 20S complex containing CDC27 and CDC16 catalyzes the mitosis-specific conjugation of ubiquitin to cyclin B. *Cell* 81: 279 – 288

Kirchner M, Renard BY, Kothe U, Pappin DJ, Hamprecht FA, Steen H, Steen JA (2010) Computational protein profile similarity screening for quantitative mass spectrometry experiments. *Bioinformatics* 26: 77 – 83

Littlepage LE, Ruderman JV (2002) Identification of a new APC/C recognition domain, the A box, which is required for the Cdh1-dependent destruction of the kinase Aurora-A during mitotic exit. *Genes Dev* 16: 2274 – 2285

Littlepage LE, Wu H, Andresson T, Deanehan JK, Amundadottir LT, Ruderman JV (2002) Identification of phosphorylated residues that affect the activity of the mitotic kinase Aurora-A. *Proc Natl Acad Sci USA* 99: 15440 – 15445

Liu Z, Yuan F, Ren J, Cao J, Zhou Y, Yang Q, Xue Y (2012) GPS-ARM: computational analysis of the APC/C recognition motif by predicting D-boxes and KEN-boxes. *PLoS One* 7: e34370

Lorca T, Castro A, Martinez AM, Vigneron S, Morin N, Sigrist S, Lehner C, Doree M, Labbe JC (1998) Fizzy is required for activation of the APC/cyclosome in Xenopus egg extracts. *EMBO J* 17: 3565 – 3575

Malik R, Lenobel R, Santamaria A, Ries A, Nigg EA, Korner R (2009) Quantitative analysis of the human spindle phosphoproteome at distinct mitotic stages. *J Proteome Res* 8: 4553 – 4563

McGarry TJ, Kirschner MW (1998) Geminin, an inhibitor of DNA replication, is degraded during mitosis. *Cell* 93: 1043 – 1053

McLachlan GJ, Basford KE (1988) Mixture Models: Inference and Application to Clustering, Vol. 84, *Statistics: Textbooks and Monographs*. New York: Marcel Dekker

Merbl Y, Kirschner MW (2009) Large-scale detection of ubiquitination substrates using cell extracts and protein microarrays. *Proc Natl Acad Sci USA* 106: 2543 – 2548

Miki H, Okada Y, Hirokawa N (2005) Analysis of the kinesin superfamily: insights into structure and function. *Trends Cell Biol* 15: 467 – 476

Mountain V, Simerly C, Howard L, Ando A, Schatten G, Compton DA (1999) The kinesin-related protein, HSET, opposes the activity of Eg5 and cross-links microtubules in the mammalian mitotic spindle. *J Cell Biol* 147: 351 – 366

Murray AW, Kirschner MW (1989) Cyclin synthesis drives the early embryonic cell cycle. *Nature* 339: 275 – 280

Murray AW, Solomon MJ, Kirschner MW (1989) The role of cyclin synthesis and degradation in the control of maturation promoting factor activity. *Nature* 339: 280 – 286

Murtag F, Raftery A (1984) Fitting straight lines to point patterns. *Pattern Recogn* 17: 479 – 483

Nakayama KI, Nakayama K (2006) Ubiquitin ligases: cell-cycle control and cancer. *Nat Rev Cancer* 6: 369 – 381

Olsen JV, Vermeulen M, Santamaria A, Kumar C, Miller ML, Jensen LJ, Gnad F, Cox J, Jensen TS, Nigg EA, Brunak S, Mann M (2010) Quantitative phosphoproteomics reveals widespread full phosphorylation site occupancy during mitosis. *Sci Signal* 3: ra3

Ozlu N, Monigatti F, Renard BY, Field CM, Steen H, Mitchison TJ, Steen JJ (2010) Binding partner switching on microtubules and aurora-B in the mitosis to cytokinesis transition. *Mol Cell Proteomics* 9: 336 – 350

Pe'er T, Lahmi R, Sharaby Y, Chorni E, Noach M, Vecsler M, Zlotorynski E, Steen H, Steen JA, Tzur A (2013) Gas2l3, a novel constriction site-associated protein whose regulation is mediated by the APC/C Cdh1 complex. *PLoS One* 8: e57532

Peters JM (2006) The anaphase promoting complex/cyclosome: a machine designed to destroy. *Nat Rev Mol Cell Biol* 7: 644 – 656

Pfleger CM, Kirschner MW (2000) The KEN box: an APC recognition signal distinct from the D box targeted by Cdh1. *Genes Dev* 14: 655 – 665

Rape M, Kirschner MW (2004) Autonomous regulation of the anaphase-promoting complex couples mitosis to S-phase entry. *Nature* 432: 588 – 595

Rape M, Reddy SK, Kirschner MW (2006) The processivity of multiubiquitination by the APC determines the order of substrate degradation. *Cell* 124: 89 – 103

Rath O, Kozielski F (2012) Kinesins and cancer. *Nat Rev Cancer* 12: 527 – 539

Reinhold WC, Erliandri I, Liu H, Zoppoli G, Pommier Y, Larionov V (2011) Identification of a predominant co-regulation among kinetochore genes, prospective regulatory elements, and association with genomic instability. *PLoS One* 6: e25991

Renard BY, Kirchner M, Monigatti F, Ivanov AR, Rappsilber J, Winter D, Steen JAJ, Hamprecht FA, Steen H (2009) When less can yield more - Computational preprocessing of MS/MS spectra for peptide identification. *Proteomics* 9: 4978 – 4984

Richardson HE, Wittenberg C, Cross F, Reed SI (1989) An essential G1 function for cyclin-like proteins in yeast. *Cell* 59: 1127 – 1133

Schmidt A, Rauh NR, Nigg EA, Mayer TU (2006) Cytostatic factor: an activity that puts the cell cycle on hold. *J Cell Sci* 119: 1213 – 1218

Sedgwick GG, Hayward DG, Di Fiore B, Pardo M, Yu L, Pines J, Nilsson J (2013) Mechanisms controlling the temporal degradation of Nek2A and Kif18A by the APC/C-Cdc20 complex. *EMBO J* 32: 303 – 314

Singh S, Kirchner M, Steen JA, Steen H (2012a) A practical guide to the FLEXIQuant method. *Methods Mol Biol* 893: 295 – 319

Singh S, Springer M, Steen J, Kirschner MW, Steen H (2009) FLEXIQuant: a novel tool for the absolute quantification of proteins, and the simultaneous identification and quantification of potentially modified peptides. *J Proteome Res* 8: 2201 – 2210

Singh SA, Winter D, Bilimoria PM, Bonni A, Steen H, Steen JA (2012b) FLEXIQinase, a mass spectrometry-based assay, to unveil multikinase mechanisms. *Nat Methods* 9: 504 – 508

Steen JAJ, Steen H, Georgi A, Parker K, Springer M, Kirchner M, Hamprecht F, Kirschner MW (2008) Different phosphorylation states of the anaphase promoting complex in response to antimitotic drugs: a quantitative proteomic analysis. *Proc Natl Acad Sci USA* 105: 6069 – 6074

Swartz G (1978) Estimating the dimension of a model. *Ann Stat* 6: 461 – 464

Tian W, Li B, Warrington R, Tomchick DR, Yu H, Luo X (2012) Structural analysis of human Cdc20 supports multisite degron recognition by APC/C. *Proc Natl Acad Sci USA* 109: 18419 – 18424

Villerbu N, Gaben AM, Redeuilh G, Mester J (2002) Cellular effects of purvalanol A: a specific inhibitor of cyclin-dependent kinase activities. *Int J Cancer* 97: 761 – 769

Wagner SA, Beli P, Weinert BT, Nielsen ML, Cox J, Mann M, Choudhary C (2011) A proteome-wide, quantitative survey of *in vivo* ubiquitylation sites reveals widespread regulatory roles. *Mol Cell Proteomics* 10: M111 – M013284

Walczak CE, Verma S, Mitchison TJ (1997) XCTK2: a kinesin-related protein that promotes mitotic spindle assembly in Xenopus laevis egg extracts. *J Cell Biol* 136: 859 – 870

Wang Z, Udeshi ND, Slawson C, Compton PD, Sakabe K, Cheung WD, Shabanowitz J, Hunt DF, Hart GW (2010) Extensive crosstalk between O-GlcNAcylation and phosphorylation regulates cytokinesis. *Sci Signal* 3: ra2

Winter D, Steen H (2011) Optimization of cell lysis and protein digestion protocols for the analysis of HeLa S3 cells by LC-MS/MS. *Proteomics* 11: 4726 – 4730

Wurzenberger C, Gerlich DW (2011) Phosphatases: providing safe passage through mitotic exit. *Nat Rev Mol Cell Biol* 12: 469 – 482

Zhao WM, Coppinger JA, Seki A, Cheng XL, Yates JR III, Fang G (2008) RCS1, a substrate of APC/C, controls the metaphase to anaphase transition. *Proc Natl Acad Sci USA* 105: 13415 – 13420

Zhu C, Zhao J, Bibikova M, Leverson JD, Bossy-Wetzel E, Fan JB, Abraham RT, Jiang W (2005) Functional analysis of human microtubule-based motor proteins, the kinesins and dyneins, in mitosis/cytokinesis using RNA interference. *Mol Biol Cell* 16: 3187 – 3199

Zou H, McGarry TJ, Bernal T, Kirschner MW (1999) Identification of a vertebrate sister-chromatid separation inhibitor involved in transformation and tumorigenesis. *Science* 285: 418 – 422